Background

Wheat (*Triticumaestivum* L) is a widely cultivated crop on over 200 million hectares with an annual production of approximately 700 million metric tons of grain (http://www.fao.org/faostat/). Wheat contributes to nearly 20% of the total dietary calories and protein consumed worldwide [1]. Raising grain yield remains the main target in wheat breeding. Manipulating plant architecture o ers an important approach for the improvement of grain yield in crops. Plant architecture encompasses branching (tillering) pattern, plant height, the shape, size, location of leaves, and reproductive organs. Plant architecture is closely associated with the adaptability of a crop to variable environments, assimilate accumulation, and harvest indexing [2]. According to Donald [3], a crop ideotype is a weak competitor and makes a minimum demand on resources per unit of dry matter produced. An ideal plant architecture is of high e ciency relative to its environmental resources. Ideal plant architecture/node length of wheat is di erent in variable environments (e.g., drought, lodging). Dwarfing and semi-dwarfing alleles of *Reduced height* (*Rht*) loci substantially reduce plant height and improve assimilate partitioning to spike and high lodging resistance, all further leading to the improvement of grain yields in wheat [4]. In wheat, plant height is determined by internode number, internode length, and spike length. New internodes are produced until the wheat plants reach the floret initiation stage. After this stage, the increase in stem length mainly reflects internode and spike elongation. us, internode initiation rate and internode and spike elongation rate during stem elongation are the major determinants for plant height. e di erent internodes of an individual stem play variable roles in determining grain yield. Combining the desired phenotype of both apical and basal internodes will be beneficial for increasing grain yield in crops.

Crop domestication and breeding induce natural allelic variations, which determine quantitative trait loci (QTLs) associated with agricultural traits. Understanding the genetic basis of phenotypic variation in various germplasm is critical for making accurate selection decisions and for combining desired allelic combinations, which will lead to the improvement of wheat grain yield. Genome-wide association studies (GWAS) o er a powerful approach for dissecting the genetic basis of complex traits and identifying causal polymorphisms [5, 6]. Although a substantial number of wheat GWAS have been reported, these studies are underpowered owing to the relatively small number of single-nucleotide polymorphisms (SNPs) used (< 1million). With the availability of the wheat reference genome and next-generation sequencing technologies for resequencing analyses, comparative genomic sequence analyses enable us to identify more than 100 million SNPs [7–14]. Haplotype analysis of the associated genomic regions may reveal the selection process of the preferred haplotype during wheat breeding. e identification and utilization of superior alleles for the associated traits may greatly facilitate the breeding of new wheat cultivars with high grain yield. e utilization of preferred haplotypes holds great potential for the improvement of wheat grain yield.

To look for the regulators that separately control the length of each internode, and assess the genetic basis of geographical di erentiation and breeding selection for wheat plant architecture traits, we conducted GWAS of eight plant architecture traits in 306 worldwide wheat accessions and determined the associated haplotypes and their geographical distribution. We further examined the breeding e ects on these haplotypes in 831 wheat

accessions that were introduced from other countries or developed in China from 1900 to 2020. Moreover, we explored a number of loci that can separately control the length of internodes within individual stems.

Overview of plant architecture traits in this study

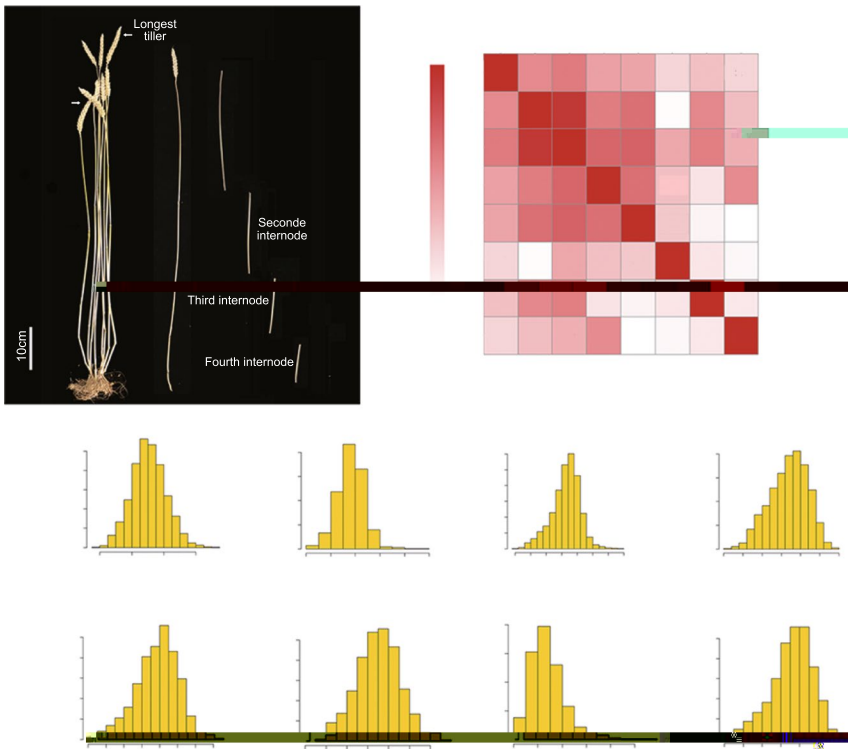

Genome-wide association studies reveal shared and independent genetic determinants of plant architecture traits

In this study, we used genotypic data of wheat accessions from the whole-genome genetic variation map of wheat (VMap [7, 14]). e latest version of VMap (VMap 2.0) [17] consists of 1062 wheat accessions with multiple ploidy levels, from which we selected 306 hexaploid wheat accessions worldwide for this study. e high coverage whole-genome sequencing ($\sim 10\times$) enabled the identification of 40,710,923 filtered SNPs with minor allele frequency (MAF) > 0.05 across the 306 wheat accessions. Based on these 40,710,923 SNPs, we performed GWAS for the phenotypic values of the eight plant architecture traits in each of the two environments (Y1, 2) and their BLUE values and identified 56,096 (Y1:20,877; Y2:23,315; BLUE:11,904) significant marker–trait associations ($-\mathrm{Log}_{10}$ (*P*-value) > 5.0) (Fig. 2a, Additional file 2: Table S3). We used linkage disequilibrium (LD) and connections between markers to delineate about 330 significantly associated loci, when at least five nearby SNPs were above the significance threshold, associated with at least one of the eight plant architecture traits (Additional file 2: Table S4). Of the 330 loci, 83 were associated with a single trait, while the remaining 247 showed pleotropic e ects on more than one

plant architecture traits (Additional file 2: Table S4). Notably, we observed that some significant loci were specially associated with the length of the four internodes, suggesting the relative independence of the genetic control of internode length in this study.

Pleiotropy and LD play important roles in validating phenotypic correlations [18]. Of the 247 loci with pleotropic effects, 182 were associated with more than four traits, and 64 loci had associations with two or three traits (Fig. 2b, Additional file 2: Table S4). These results suggest that these traits might be genetically co-regulated. We took *TEOSINTE BRANCHED1* (*TB1*) as a control, because recent work reported that *TB1* regulates height and stem internode length in bread wheat [19]. The genomic region (Chr4D: 15,938,883-19,054,796) including *TB1* was associated with the length of second internode, third internode, shortest tiller, longest tiller, and main shoot (Additional file 2: Table S5), suggesting its potential connection with internode length, which is consistent with previous finding [19]. Notably, the major loci for the length of the main shoot (Y1-MSL-1A-1; 2,891 associated SNPs; B-MSL-1A-1:391 associated SNPs), the longest tiller (Y1-LTL-1A-1; 6,079 associated SNPs; B-LTL-1A-1: 27 associated SNPs), the shortest tiller (Y1-STL-1A-1: 1002 associated SNPs; B-STL-1A-1: 5 associated SNPSs), and the peduncle (Y1-PL-1A-1: 5,768 associated SNPs; B-PL-1A-1: 396 associated SNPS; Y2-PL-1A-1: 4 associated SNPs) located in chromosome 1A: 45,791,400-49,172,693 (Additional file 2: Table S4). Most loci for the length of the longest and the shortest tillers overlapped, thus explaining the strong phenotypic correlations between peduncle length and tiller length as well as the consistency of the length among the tillers of individual plants.

To confirm the selected loci in the wheat genome during the gradual improvement of grain yield in China, we selected 59 Chinese wheat accessions (17 cultivars versus 42 landraces) from the 306 wheat accessions for further analysis. These 59 Chinese accessions were selected to display the genomic selection during Chinese wheat breeding process, which will be further used to examine the selection of the associated peaks identified by GWAS. The 59 Chinese accessions are important varieties during Chinese wheat breeding process. We combined the results of whole-genome differentiation of the cross-population composite likelihood ratio (XP-CLR) (Fig. 2c, Additional file 2: Table S6). In total, we determined that 49% of the detected loci (163 of 330) during this study were significantly selected in wheat improvement for higher yield (Fig. 2c, Additional file 2: Table S4). The loci associated with the length of the main shoot, the second internode length, and the longest and shortest tiller in this study (e.g., Y1-MSL-2A-7, Y2-MSL-6B-1, Y2-SIL-2A-1, Y1-SIL-2A-2,, Y2-STL-2A-1, and Y1-LTL-2A-1) as well as known plant height genes (e.g., *Rht-D1*, and *Rht8*) appeared to have experienced a strong selective sweep (Additional file 2: Tables S4 and S6). Moreover, the loci that are specifically associated with the length of the peduncle, and the third and fourth internodes (Y1-PL-1A-1

Rht-D1) associated with spike development, and grain number and size were under strong selection (Additional file 2: Table S6). This result reflected the improvement of adaptation to local environments and grain yield in wheat breeding.

Genetic basis of geographical differentiation and breeding selection of internode length

The internodes within individual stems play different roles in determining grain yield in crops. To search for loci that can separately regulate the length of the four internodes and determine the genomic basis of geographical differentiation and breeding selection for these traits, we examined the distribution of internode length as a function of the geographical provenance of each accession. We then examined the proportion of each haplotype in all geographical regions based on the four major loci specifically associated with the length of each of the four internodes (Fig. 2a, Additional file 2: Table S1) in the 306 worldwide wheat accessions. In addition, we characterized the extent and direction of the changes of haplotype composition in the 831 wheat accessions (most of the 831 Chinese accessions are modern cultivars) that were introduced from other countries or developed in China since 1900 (Additional file 2: Table S7). The genetic control of agronomical traits might be best understood by comparing a progenitor organism with its derivatives. Genetic crosses between progenitor and derivatives would identify the genetic factors that accounted for their different phenotypes. Thus, we examined the haplotype distribution in the wheat accessions in the two pedigrees between the 1920s and 1970s in China.

Peduncle length

Peduncle (the first internode below spike) length showed a distinct distribution pattern across the seven continents/regions (Fig. 3a, Additional file 2: Table S8). European accessions had the longest peduncles (52.88 cm), whereas Asian accessions had the shortest peduncles (46.83 cm) (Fig. 3a, Additional file 2: Table S8). The major locus (Y1-PL-1A-1(5768 associated SNPs); B-PL-1A-1(396 associated SNPs); Y2-PL-1A-1 (four associated SNPs) associated with peduncle length mapped to chromosome 1A:45,791,400-49,094,709. We identified three haplotypes of this locus (peduncle length-long, PL-L; peduncle length-medium, PL-M; peduncle length-short, PL-S) in the 306 worldwide wheat accessions: Hap^{PL-S} = 49.27 cm (48.37% of accessions), Hap^{PL-M} = 48.83 cm (20.26% of accessions), Hap^{PL-L} = 53.84 cm (31.37% of accessions) (Fig. 3b, c, Additional file 2: Tables S9 and S10). European accessions exhibited a higher proportion of Hap^{PL-L}, whereas Hap^{PL-S} and Hap^{PL-M} was more heavily represented in Asian accessions (Fig. 3b, c, Additional file 2: Table S10). In addition, within each of the three haplotypes, the European accessions always had a longer peduncle than African accessions (Additional file 2: Table S10). These results revealed the genetic basis of the differences in peduncle length between geographical areas.

The genomic region covering Y1-PL-1A-1 was under clear selection between Chinese landraces and cultivars (Fig. 3d). To further assess the selection of Y1-PL-1A-1 in Chinese wheat accessions over the past 120 years, we determined the proportion of each haplotype in 831 wheat accessions that were introduced from other countries or developed in China since 1900 (Fig. 3e, Additional file 2: Table S7). In the 831 wheat

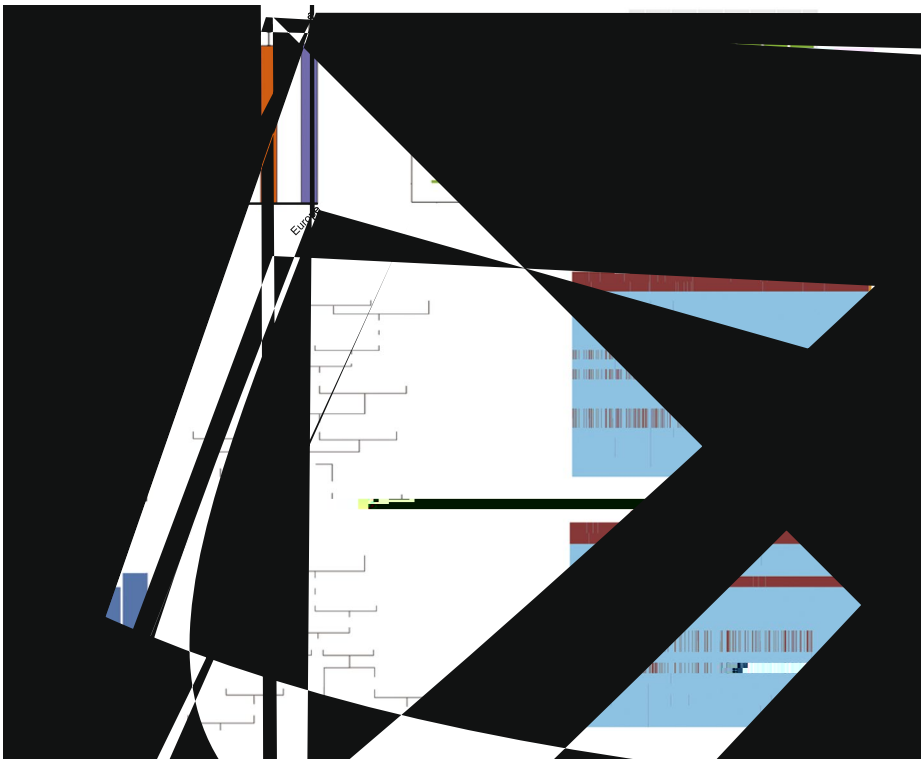

accessions, Hap^{PL-M} was the major haplotype (67%, 553 of 831 accessions), whose relative frequency increased from 41% before 1960 to 75% in the time window of 2001–2020. e other two haplotypes, Hap^{PL-S} and Hap^{PL-L}, were present in the 200 and 15 Chinese wheat accessions, respectively, indicating that the haplotype Hap^{PL-L} has not been widely used in China. In agreement with this observation, plants including peduncles have become shorter in China over the past 120 years. e dynamics in haplotypes reflected the genomic scale of breeding selection in China over the past 120 years.

To confirm the changes in frequency for the haplotypes at Y1-PL-1A-1, we used two important pedigrees (Aimengniu, Xiaoyan6) in Chinese wheat breeding. We examined the breeding histories of two important cultivars (Aimengniu, Xiaoyan6) that

were initially released in the early 1980s. Aimengniu is a high yield variety, which is the founder genotype for more than 20 released Chinese cultivars, many of which are widely planted in China [9]. Xiaoyan6 was recognized through an award in 1985, and more than 40 Chinese cultivars have been derived from this founder genotype [9]. Our collection included a variety of pedigree contributors and subsequently released derived cultivars for both Aimengniu and Xiaoyan6 founder genotypes (Fig. 3f, h). e genetic contribution of founder genotypes to their derived cultivars was reported in our previous work [9]. We examined the distribution of three haplotypes (Hap^{PL-S}, Hap^{PL-M}, and Hap^{PL-L}) in the two pedigrees of two founder genotypes (Aimengniu, Xiaoyan6) (Fig. 3f, h). Both pedigrees were ultimately derived from three major global genotypes (Rieti, Wilhelmina, and Akagomughi) between the 1920s and 1970s [9]. In the first pedigree (Aimengniu), three founder genotypes (Rieti, Wilhelmina, and Akagomughi) contributed to derived cultivars: Mentana, Autonomia, Abbondanza, Mengxian 201, Aimengniu. More recently, Zhoumai 9, Zhoumai 16, Xumai 35, Zhoumai 18, and Zhongmai 66 derived from Aimengniu (Fig. 3f). In addition, some other varieties (e.g., Fontarronco, Yuejin5, Neuzucht, Aifeng5, Bainong791, Yanshi4, Zhou8425B) contributed to derived cultivars in the first pedigree. In the second pedigree (Xiaoyan6), Villa Glori, San Pastore, St 2422/464, and Xiaoyan6 were the derivatives of the same founder genotypes (Rieti, Wilhelmina, and Akagomughi). Next, Xinong 881, Zhengmai 9023, Zhengmai 366, Xinong 979, and Fengdecunmai 5 derived from Xiaoyan6 (Fig. 3h). Moreover, some other varieties (e.g. Mara, Xiaoyan96, Xinong65, Yumai47, Shaan 213, Zhengmai16) contributed to derived cultivars in the second pedigree (Xiaoyan6). All the SNP information of the varieties in the two pedigrees can be obtained from our previous work [9].

e haplotype distribution in the wheat accessions in the pedigrees allowed us to identify the haplotypes that matched the modification of wheat breeding (Fig. 3g, i, Additional file 2: Tables S11 and S12). In the two pedigrees, for the three original founder genotypes, Rieti, Wilhelmina, and Mara harbored Hap^{PL-L}, while Akagomughi carried the Hap^{PL-S} (Fig. 3g, i). e remaining derived cultivars had Hap^{PL-S}, except Mengxian 201 (first pedigree), Neuzucht (first pedigree), Aimengniu (first pedigree), Yanshi4 (first pedigree), Yumai47 (second pedigree), Zhengmai366 (second pedigree), and Fengdecunmai5 (second pedigree) with Hap^{PL-M} (Fig. 3g, i, Additional file 2: Tables S11 and S12). e di erent haplotypes of these four derivatives with the three original founder genotypes also indicated the contribution of other founder genotypes. is finding was consistent with reduced plant height in wheat breeding. However, we cannot exclude the possibility that Hap^{FIL-S} was likely introduced from other founders which does not belong to these two pedigrees.

Length of the second internode

Oceanian accessions exhibited the longest second internode of all groups (30.11 cm), whereas African accessions had the shortest second internode (26.71 cm) (Additional file 2: Table S8, Additional file 1: Fig. S2a). e major locus (Y1-SIL-1A-2) associated with the length of second internode located to chromosome 1A:555,809,177-557,861,830. We detected two haplotypes at this locus (second internode length-long, SIL-L; second internode length-short, SIL-S) in the 306 worldwide wheat accessions: $Hap^{SIL-L} = 28.61$ cm (94.44% of accessions), $Hap^{SIL-S} = 22.93$ cm (4.90% of accessions)

(Additional file 2: Tables S9 and S10; Additional file 1: Fig. S2b, c). All Oceanian accessions harbored only Hap^{SIL-L}, whereas African accessions presented both Hap^{SIL-L} (89.66%) and Hap^{SIL-S} (10.34%) (Additional file 2: Table S10; Additional file 1: Fig. S2b, c). The distinct distribution of the two haplotypes supported the genomic basis of the phenotypic differences between Oceania and Africa.

The locus Y1-SIL-1A-2 was not a target of selection between Chinese landraces and cultivars (Additional file 2: Table S4; Additional file 1: Fig. S2d). Indeed, we only detected one haplotype (Hap^{SIL-L}) across the 831 wheat accessions, making Hap^{SIL-S} absent from Chinese wheat accessions (Additional file 1: Fig. S2e). We examined the haplotype distribution in the two pedigrees, as shown in Fig. 3e, g (Additional file 2: Tables S11 and S12; Additional file 1: Fig. S2f, g). For the three original founder genotypes, Rieti and Wilhelmina carried Hap^{SIL-L}, and Akagomughi harbored the Hap^{SIL-S}. Importantly, no derivatives in either pedigrees retained Hap^{SIL-S}, except Yuejin5 (first pedigree) and Zhou8425B (first pedigree), indicating that Hap^{SIL-S} was selected against these derivatives (Additional file 2: Tables S11 and S12; Additional file 1: Fig. S2f, g), in agreement with its absence in the 831 wheat accessions.

Length of the third internode

Middle Eastern accessions had the longest third internode (23.08 cm), whereas Oceanian accessions exhibited the shortest third internode (19.69 cm) (Additional file 2: Table S8; Additional file 1: Fig. S3a). The major locus (Y1-TIL-3D-1) associated with third internode length mapped to chromosome 3D:35,786,271-39,382,820. We identified two haplotypes at this locus (third internode length-long, TIL-L; third internode length-short, TIL-S) in the 306 worldwide wheat accessions: $Hap^{TIL-S} = 21.57$ cm (94.10% of accessions), $Hap^{TIL-L} = 21.87$ cm (5.90% of accessions) (Additional file 2: Tables S9 and S10; Additional file 1: Fig. S3b, c). Although we did not observed significant difference of the BLUE values of data in 2021 and 2022, the phenotypic values for these two haplotypes were obviously different for each year (Additional file 2: Table S13). Middle Eastern accessions had the (88.10% of accessions) and Hap^{TIL-L} (11.90% of accessions) Hap^{TIL-S} haplotype, whereas African accessions presented both Hap^{TIL-S} (93.10% of accessions) and Hap^{TIL-L} (6.90% of accessions) (Additional file 2: Table S10, Additional file 1: Fig. S3b, c). The differences of the distribution of the two haplotypes indicated the genomic basis of the phenotypic differences between Africa and the Middle East.

We determined that Y1-TIL-3D-1 was selected between Chinese landraces and cultivars (Additional file 2: Table S4, Additional file 1: Fig. S3d). Indeed, the frequency distribution of Y1-TIL-3D-1 haplotypes changed over time. While Hap^{TIL-S} was the major haplotype in the 831 wheat accessions, its frequency increased from 90% before 1960 phase to 96% after 2000 (Additional file 2: Table S7; Additional file 1: Fig. S3e). In the two pedigrees, all the wheat accessions had Hap^{TIL-S} (Additional file 2: Tables S11 and S12; Additional file 1: Fig. S3f, g).

Length of the fourth internode

Middle Eastern accessions had the longest fourth internode (18.23 cm), whereas African accessions had the shortest fourth internode (14.52 cm) (Additional file 2: Table S8; Additional file 1: Fig. S4a). The major locus (Y1-FIL-2A-3; B-FIL-2A-1) associated with

fourth internode length located to chromosome 2A:613,558,313–619,417,320. We detected two haplotypes at this locus (fourth internode length-long, FIL-L; fourth internode length-short, FIL-S) in the 306 worldwide wheat accessions: $Hap^{FIL-L} = 17.54$ cm (90.82%), Hap^{FIL-S}

one free-threshing tetraploid B016 turns out to be the most possible donor of Mengxian201, because it has the most similar haplotype blocks with Mengxian201 among all five candidates and f_d values are nearly equal to 1 across the locus (Fig. 4c, d). Furthermore, the minimum IBS distance also support this hypothesis, the value of IBS distance between Mengxian201 and B016 is even smaller than that with the hexaploid landrace Aifeng3 (Fig. 4c). Our work indicated that free-threshing tetraploids B016 is the most possible donor of Mengxian201; however, it might not be the direct donor, since we cannot exclude the other possibilities during wheat breeding, such as natural outcrossing, heterozygous parent.

We observed obvious di erences of the phenotypic values between the two environments for the length of four internodes (Additional file 2: Table S2). Notably, the genotypic values for the length of the first and second internodes were higher in 2021 than those in 2022. However, the genotypic values for the length of the third and fourth internodes were higher in 2022 than those in 2021. e Shukla model [21] was used to evaluate the interaction between genotypes and environments (Additional file 2: Table S14). Obvious interactions between haplotypes and environments for four haplotypes (Hap^{PL-S}, Hap^{SIL-L}, Hap^{SIL-S}, Hap^{TIL-L}) were observed in this study (Additional file 2:

Table S14). In addition, the results suggested the relative stability of other haplotypes of the length of four internodes (Additional file 2: Table S14).

Genomic basis of geographical di erentiation of tiller length

We identified a locus on chromosome 1A between 45,791,400 and 49,172,693 bp that was associated with the length of the longest tiller, the shortest tiller, and the main shoot.

is locus mapped to the same position as the major locus of the first internode length mentioned above (Additional file 2: Table S4). We observed the highest values for the longest tiller, shortest tiller, and the main shoot in European wheat accessions and the shortest values in African wheat accessions, which was the same trend as that seen for the length of the first internode (Additional file 2: Table S8). Similarly, the three haplotypes associated with the locus for first internode length displayed identical e ects on the length of the longest tiller, shortest tiller, and the main shoot (Additional file 2: Table S10), suggesting that this observed haplotype distribution might explain the geographical distribution of these phenotypes.

Geographical di erentiation and breeding selection of haplotype combinations for the length of the internodes

Wheat breeding has exploited variable haplotypes associated with agricultural traits. Understanding the genetic basis of this phenotypic variation in various germplasms is critical for making accurate selection decisions and for combining desired haplotype combinations to improve wheat grain yield. We detected seven major haplotype combinations of the four major loci for the length of the four internodes. ese seven combinations accounted for 94.12% (288 accessions) of all the haplotypes in the 306 worldwide wheat accessions (Additional file 2: Table S16). We determined the e ects of the seven combinations on the associated traits (Fig. 5a–d, Additional file 2: Table S17).

e four internodes were shorter in haplotype combination 4 (C4, Hap

from 26.05% of all accessions before 1960 to 13.33% (1961–1980), 7.22% (1981–2000), and 3.98% (2001–2020) (Fig. 5h, Additional file 2: Table S18). e haplotype combination (Hap^{PL-M}-Hap^{SIL-L}-Hap^{TIL-S}-Hap^{FIL-N1}) increased obviously in frequency from pre-1961 to 1961–1980 among Chinese wheat accessions, suggesting that this combination was selected during this time window (Fig. 5i, Additional file 2: Table S18). Similarly, another haplotype combination (Hap

D

Plant breeders have paid special attention to plant architecture for decades because of its significance for improving varieties. Plant architecture plays a decisive role in grain yield potential. Plants with reduced height benefit from improved lodging resistance and assimilates partitioning to the developing spike, facilitating improved floret fertility and grain numbers per spike [22].

Some QTLs and genes associated with internode length have been identified in different species, which provided genetic resources for the manipulation of plant height through the length of di erent internodes [23–28]. To the best of our knowledge, in wheat, some genetic work related to peduncle have been reported [29, 30]. However, few genetic studies dissected the length of internodes or the length of the shortest and longest tillers within individual plants. e only publication reported the QTLs of the internode length using two biparental populations without the physical positions in wheat genome, since the information of reference genome was not available at that time [31]. Some identified loci in this study were overlapped with reported QTLs or genes in previous work. Nevertheless, a big proportion of the identified loci, especially these loci associated with four internodes, are novel relative to previous studies.

In this study, we determined the phenotypic variation for eight plant architecture traits, including the length of the four internodes and the shortest and the longest tiller, based on 306 worldwide wheat accessions originating from the seven continents/regions. We used whole-genome sequencing data for these 306 wheat accessions, with an average depth of $10\times$ coverage and identified about 40 million high-confidence and high-quality SNPs. GWAS results identified QTLs that are independent of the known *Rht* genes, therefore providing new resources for the genetic control of plant height and internode length.

Few studies have explored the genetic basis of the geographical distribution and breeding selection of the internode length. In this study, the worldwide distribution of the haplotypes underlying each of the identified QTLs o ers a glimpse into the genomic basis behind the phenotypic di erences for the eight traits measured here as a function of geographical origin. In addition, we examined the selection of all haplotypes during wheat over the past 120 years in China. ese haplotypes have been clearly selected (for or against) in Chinese breeding, indicating that the observed alterations of haplotypes underscore the genomic basis of modification for plant architecture traits in the past 120 years in China.

e peduncle, the first internode below the spike, plays variable roles in the determination of crop grain yield. e peduncle vascular system is critical for the transport of photosynthetic products, nutrients, and water from the roots and leaves to the filling grain [32, 33]. We identified one major locus related to the length of peduncle and main shoot. Within this major locus, four SNPs were significantly ($-\mathrm{Log}_{10}[P\text{-value}] > 5.0$) associated with the traits and located in the gene *TraesCS1A02G064800*. erefore, we identified *TraesCS1A02G064800* as a candidate gene that controlled peduncle length. e orthologue of *TraesCS1A02G064800* in Arabidopsis is *Trehalose-6-P synthase 1*. We identified four major haplotypes at *TraesCS1A02G064800* in the 306 worldwide wheat accessions (Fig. 6c, Additional file 2: Table S19). ese four haplotypes comprised 59, 93, 88, and 53 accessions,

respectively (Additional file 2: Table S19). We determined the e ects of the four haplotypes on the associated traits (Fig. 6d, e, Additional file 2: Table S16). ere were significant di erences in the length of the peduncle (main shoot) and the main shoot between these four haplotypes (Fig. 6d, e, Additional file 2: Table S16). erefore, we identified *TraesCS1A02G064800* as a candidate gene that controlled the length of peduncle and main shoot.

To compare the contributions of *TraesCS1A02G064800* alleles to the length of peduncle and the main shoot and evaluate its potential value in wheat breeding, we assessed the phenotypic di erences of these two traits between the alleles in a genetic population. Sequencing the coding sequence (CDS) of *TraesCS1A02G064800* resulted in the identification of a nonsynonymous A/G SNP (4,245 bp into the gene, 1,046 bp in the coding sequence) between the cultivars Zhongmai175 (AA, average main shoot length of 71.50 cm, average peduncle length of 43.00 cm) and Yanzhan4110 (GG, average main

two alleles were present almost equally in the remaining five areas (Additional file 2: Table S20).

We examined recombinant inbred lines (RILs) generated from the parents Zhongmai175 (AA, $RILs^{long}$) and Yanzhan4110 (GG, $RILs^{short}$). On average, the $RILs^{long}$ (average plant height 70.46 cm, average peduncle length 26.22 cm) had taller plants than the $RILs^{short}$ (average plant height 66.79 cm, average peduncle length 24.84 cm) (Fig. 5g, Additional file 2: Table S21). ese results suggested the pos7(s)-5.9(e r)6(e)-7(sul-(t hei)3voT9618(dun,97

with equal spacing are evenly distributed. ese steel columns are thick at the top and thin at the bottom and have equal length, which allowed us to ensure that the hole depth is consistent.

e phenotypic data of the eight traits exhibited di erences and similarity between the two locations, and closely correlated with each other (Additional file 2: Table S11). All field management tasks (e.g., irrigation, weed management, and fertilization) were performed according to the normal standards. Plants were irrigated when required. Seven traits were measured at physiological maturity, and the resulting values were used to calculate one trait (the di erence between the length of the shortest and longest tiller). Five plants were randomly selected as five replicates for each accession to determine the eight traits at each location. e eight traits include the length of the first (peduncle), second, third, and fourth internode from top; the length of the shortest main shoot and the longest main shoot; and the di erence between the length of the shortest and the longest tiller. e main shoot was selected as the strongest tiller for each plant. e longest and shortest tillers were determined by the length of fertile tillers with spikes for individual

Genome wide association study (GWAS)

e GWAS was performed for eight plant architecture traits on 306 worldwide wheat accessions using 40,710,923 SNPs (MAF > 0.05; missing rate < 20%; missing genotype rate < 10%). e algorithm e cient mixed model association expedited (EMMAX) can e ciently correct for a wide range of population structures, which would otherwise lead to spurious genotype–phenotype associations in a GWAS [47]. erefore, the GWAS was conducted using GEMMA (version 0.98.4) by fitting the mixed linear model (MLM) association expedited (EMMAX) algorithm, including kinship as a correlation matrix.

e top three principal components (PCs) from principal component analysis (PCA) were used to build the matrix for population structure correction using Plink [48] with the parameters in the program set to "–pca 10". e matrix of simple matching coefficients was used to build the kinship (*K*) matrix. Genetic relationship between accessions was modeled as a random e ect using the *K* matrix. We used significant *P*-value thresholds ($P < 10^{-5}$) to control genome-wide type I errors according to previous study that included identical SNP number in wheat [9].

Linkage disequilibrium analysis

To determine the genomic regions of interest, the SNPs associated with all traits above a significance threshold of $-\mathrm{Log}_{10}(P\text{-value}) = 5$ were combined and the duplicates removed with vcftools. LD between SNPs was calculated by PLINK [48], with the parameters in the program set to " --allow-no-sex --maf 0.05 --geno 0.2 --r2 --ld-window 50000 --ld-window-r2 0." e results were used to combine SNPs to define intervals based on the LD between markers, with markers with $r^2 > 0.1$ being included in the same interval. If the distance between the peak SNPs of two adjacent loci was less than 5 Mb, these two loci were merged. e number of significant SNPs contained within each genomic region was counted. If the SNP number in the corresponding genomic region was more than 5, the region was defined as a QTL. e software *LDBlockShow* was used to conduct the pairwise LD analysis of the associated genomic region for *TraesCS1A02G064800* [49].

Construction of association networks

e analysis of association network was conducted using the software *Cytoscape* [50] (Version: 3.2.1). e network displayed the connections between the traits and their corresponding loci as well as the links between loci (average $r^2 \geq 0.5$). e e ective scores for each locus are represented by *P*-values of the most significant SNPs associated with the corresponding traits in the GWAS. e link between pairs of loci was represented as their average LD. Here, the LD was calculated according to previous work [6] as follows:

$$= / *(\quad (, \quad , , \quad)/ \ . \ \mathrm{ax} \quad (, \quad)+ \quad (, \quad \mathrm{n} , \quad)/ \ . \ \mathrm{ax} \quad (, \quad))$$

with LD (locus1, locus2) being the average pairwise LD value (r^2) between all SNPs of locus1 and all SNPs of locus2; PmaxLD(locus1)/PmaxLD(locus2) is the largest possible LD value within the locus1/locus2 locus, obtained by calculating the average r^2 of each SNP against all SNPs from the locus1/locus2 locus. e maximum average LD value represents this locus's PmaxLD. Pairwise r^2 values were calculated between all significant SNPs using PLINK [48].

SNP-based haplotype construction for loci

e SNP-based haplotype construction for each locus was evaluated using the *LDheatmap* and *Pheatmap* software package in R. e *Pheatmap* package defines haplotype blocks and provides the number of haplotypes and their physical length (bp) for each block, as well as the number of tagged SNPs. If the SNP was the same as in the reference type (Chinese Spring), it was given a value of 0; if the SNP was di erent from that of Chinese Spring, it was given a value of 1. Heterozygous and missing SNP were given a value of 0.5. Full cluster analysis was performed on all accessions using Euclidean distance using *Pheatmap* (version1.0.12) in R. e *LDheatmap* package in R [51] was used to conduct LD analysis for each locus in this study.

Identi cation of putative selective sweeps

e XP-CLR test [52] was used to detect selective sweeps to identify potential selective signals between Chinese cultivars (17 accessions) and landraces (42 accessions, reference population) in 306 word wheat accessions. e XP-CLR score between two wheat populations was calculated using the parameters "--ld 0.95 --maxsnps 1000 --size 50000 --step 20000." To detect which gene was under selection, the selection sweeps were ranked based on decreasing XP-CLR scores, and the top 5% regions were chosen as selective sweeps.

The interaction between genotypes and environments, and the stability of haplotypes

e Shukla model [21] was used to evaluate the interaction between genotypes and environments. e interaction evaluated using the formula as follows:

$$ge_{ij} = y_{ij} - g_i - e_j - \mu$$

where ge_{ij} is the interaction between genotypes and environemts, y_{ij} is the phenotypic values of genotype i in environment j, g_i is the e ects of genotype i, e_j is the e ects of environment j, and μ is the mean of the corresponding traits for all the genotypes in all the environments.

The *f* statistic analysis

e f_d statistic can estimate the proportion of introgression in a given window [53]. We estimated the f_d values across the genome using the python code available at https://github.com/simonhmartin/genomics_general. e sliding window was set with a window size of 100 SNPs and a step size of 5 SNPs. We converted the f_d statistic value to 0 for windows of $D<0$ because the negative f_d statistic value is meaningless. We estimated the f_d statistic value using Indian dwarf wheat as P1, Mengxian201 as P2, rye as outgroup in four-taxon topology ((P1, P2), P3, O), the P3 are diploid and tetraploid relatives of bread wheat, including 28 urartu, 31 wild einkorn, 31 domesticated einkorn, 26 wild emmer, 29 domesticated emmer, 41 free-threshing tetraploids.

The online version contains supplementary material available at https://doi.org/10.1186/s13059-023-02932-x.

Additional file 1: Figure S1. Phylogenetic relationships and population structures. **Figure S2.** Geographical distribution and breeding selection of the haplotype blocks associated with the length of the second internode on chromosome 1A. **Figure S3.** Geographical distribution and breeding selection of the haplotype blocks associated with the length of the third internode on chromosome 3D. **Figure S4.** Geographical distribution and breeding selection of the haplotype blocks associated with the length of the fourth internode on chromosome 2A. **Figure S5.** The evolutionary relationship of the haplotypes for the loci for the length of second internode, third internode, four internode.

Additional file 2: Table S1. Summary of the 306 worldwide wheat accessions. **Table S2.** Comparison of the eight plant architecture traits between two environments. **Table S3.** Detailed information of all significantly associated SNPs for the investigated traits> 5). **Table S4.** The 330 identified loci associated with investigated traits in this study. **Table S5.** Overlap between the known genes/QTLs and 330 identified loci in this study. **Table S6.** XP-CLR scores for the known genes. **Table S7.** The haplotypes of four major loci for the length of the four internodes in 831 Chinese wheat accessions. **Table S8.** The phenotypic data for the varieties from the seven continents/regions. **Table S9.** The phenotypic data of the haplotypes of the four major loci for the length of the four internodes. **Table S10.** The distribution of haplotypes of the four internodes in 306 worldwide accessions. **Table S11.** The genotypic data of all the varieties in the first pedigree. **Table S12.** The genotypic data of all the varieties in the second pedigree. **Table S13.** The interaction between environments and haplotypes for the length of the four internodes. **Table S14.** The interaction between environments and haplotypes for the length of the four internodes. **Table S15.** The 432 wheat varieties used for the analysis of the evolutionary relationship of the haplotypes. **Table S16.** The haplotype combinations for the length of the four internodes in 306 worldwide wheat accessions. **Table S17.** The haplotype combinations for the length of the four internodes in 306 worldwide wheat accessions. **Table S18.** The distribution of haplotype combinations for the length of the four internodes in 831 Chinese wheat accessions. **Table S19.** The phenotypic data of the four major haplotypes of TraesCS1A02G064800 in 306 worldwide wheat accessions. **Table S20.** The allele distribution of the SNP used in the RILs in the 306 worldwide wheat accessions. **Table S21.** The phenotypic data of RILs.

Additional file 3. Review history.

Acknowledgements
We thank Dr. Dongdong Li and Dr. Shuqin Jiang (College of Agronomy and Biotechnology, China Agricultural University, Beijing, China) for the suggestions of data analyses.

Review history
The review history is available as Additional file 3.

Peer review information
Wenjing She was the primary editor of this article and managed its editorial process and peer review in collaboration with the rest of the editorial team.

Authors' contributions
Z.G. initiated the project. Z.G., F.L., and Y.H. designed and supervised the experiments. Y.L., A.B., X.Z., D.X., X.Z, and C.H. performed sequencing and genomic-variant calls. Y.L., K.S., and J.D carried out GWAS analysis, haplotype analysis, and functional validation. Y.L., C.Y., Z.W., H.W., K.S., J.W., X.Y., Z.S., B.Y., D.L., L.Z., and L.S. conducted field experiments and phenotyping. X.X., Y.H., and Z.H. developed the genetic populations. Y.L. plotted manuscript figures. All authors were involved in

P, .[(].9961ions)]TJ /Tof all arie999618(ypes o8cesT1_4 1 Tf [(T)6 w)7(7(node)10(.)]TJ /T1)-8Tf [(T)6((ed in)]TJ d4 1 Tfloadedn continents/r)35(WT1_4J 0T)69961b

ele phenotypic ddon of all signifi7tly associated

25. Sato-Izawa K, Nakamura S, Matsumoto T. Mutation of rice bc1 gene a□ects internode elongation and induces delayed cell wall deposition in developing internodes. Plant Signal Behav. 2020;15:1–8.
26. Gomez-Ariza J, Brambilla V, Vicentini G, Landini M, Cerise M, Carrera E, Shrestha R, Chiozzotto R, Galbiati F, Caporali E, et al. A transcription factor coordinating internode elongation and photoperiodic signals in rice. Nat Plants. 2019;5:358–62.
27. Smith HMS, Hake S. The interaction of two homeobox genes, BREVIPEDICELLUS and PENNYWISE, regulates internode patterning in the Arabidopsis inflorescence. Plant Cell. 2003;15:1717–27.
28. McKim SM. Moving on up - controlling internode growth. New Phytol. 2020;226:672–8.
29. Gaur A, Jindal Y, Singh V, Tiwari R, Kumar D, Kaushik D, Singh J, Narwal S, Jaiswal S, Iquebal MA, et al. GWAS to identify novel QTNs for WSCs accumulation in wheat peduncle under di□erent water regimes. Front Plant Sci. 2022;13:825687.
30. Govta N, Polda I, Sela H, Cohen Y, Beckles DM, Korol AB, Fahima T, Saranga Y, Krugman T. Genome-wide association study in bread wheat identifies genomic regions associated with grain yield and quality under contrasting water availability. Int J Mol Sci. 2022;23:10575–97.
31. Cui F, Li J, Ding AM, Zhao CH, Wang L, Wang XQ, Li SS, Bao YG, Li XF, Feng DS, et al. Conditional QTL mapping for plant height with respect to the length of the spike and internode in two mapping populations of wheat. Theor Appl Genet. 2011;122:1517–36.
32. Wardlaw IF. Tansley review no. 27 The control of carbon partitioning in plants. New Phytol. 1990;116:341–81.
33. Kong LA, Wang FH, Feng B, Li SD, Si JS, Zhang B. The structural and photosynthetic characteristics of the exposed peduncle of wheat (*Triticum aestivum* L.): an important photosynthate source for grain-filling. BMC Plant Biol. 2010;10:141–50.
34. Liu C, Zheng S, Gui JS, Fu CJ, Yu HS, Song DL, Shen JH, Qin P, Liu XM, Han B, et al. Shortened basal internodes encodes a gibberellin 2-oxidase and contributes to lodging resistance in rice. Mol Plant. 2018;11:288–99.
35. Schrager-Lavelle A, Gath NN, Devisetty UK, Carrera E, Lopez-Diaz I, Blazquez MA, Maloof JN. The role of a class III gibberellin 2-oxidase in tomato internode elongation. Plant J. 2019;97:603–15.
36. Peltonen-Sainio P, Kangas A, Salo Y, Jauhiainen L. Grain number dominates grain weight in temperate cereal yield determination: evidence based on 30 years of multi-location trials. Field Crop Res. 2007;100:179–88.
37. Shearman VJ, Sylvester-Bradley R, Scott RK, Foulkes MJ. Physiological processes associated with wheat yield progress in the UK. Crop Sci. 2005;45:175–85.
38. Ma LY, Bao J, Guo LB, Zeng DL, Li XM, Ji ZJ, Xia YW, Yang CD, Qian Q. Quantitative trait loci for panicle layer uniformity identified in doubled haploid lines of rice in two environments. J Integr Plant Biol. 2009;51:818–24.
39. Zhao CH, Zhang N, Wu YZ, Sun H, Liu C, Fan XL, Yan XM, Xu HX, Ji J, Cui F. QTL for spike-layer uniformity and their influence on yield-related traits in wheat. BMC Genet. 2019;20:23–33.
40. Zhou KY, Lin Y, Jiang XJ, Zhou WL, Wu FK, Li CX, Wei YM, Liu YX. Identification and validation of quantitative trait loci mapping for spike-layer uniformity in wheat. Int J Mol Sci. 2022;23:1052–63.
41. Bates D, Machler M, Bolker BM, Walker SC. Fitting linear mixed-e□ects models using lme4. J Stat Softw. 2015;67:1–48.
42. Sun C, Dong Z, Zhao L, Ren Y, Zhang N, Chen F. The Wheat 660K SNP array demonstrates great potential for marker-assisted selection in polyploid wheat. Plant Biotechnol J. 2020;18:1354–60.
43. Shi S, Yuan N, Yang M, Du ZL, Wang JY, Sheng X, Wu JY, Xiao JF. Comprehensive assessment of genotype imputation performance. Hum Hered. 2017;83:107–16.
44. Browning BL, Zhou Y, Browning SR. A one-penny imputed genome from next-generation reference panels. Am J Hum Genet. 2018;103:338–48.
45. Browning BL, Tian XW, Zhou Y, Browning SR. Fast two-stage phasing of large-scale sequence data. Am J Hum Genet. 2021;108:1880–90.
46. Wang W, Wang Z, Li X, Ni Z, Hu Z, Xin M, Peng H, Yao Y, Sun Q, Guo W. SnpHub: an easy-to-set-up web server framework for exploring large-scale genomic variation data in the post-genomic era with applications in wheat. Gigascience. 2020;9:1–8.
47. Kang HM, Sul JH, Service SK, Zaitlen NA, Kong SY, Freimer NB, Sabatti C, Eskin E. Variance component model to account for sample structure in genome-wide association studies. Nat Genet. 2010;42:348–54.
48. Gao F, Ming C, Hu WJ, Li HP. New software for the fast estimation of population recombination rates (FastEPRR) in the genomic era. G3. 2016;6:1563–71.
49. Dong SS, He WM, Ji JJ, Zhang C, Guo Y, Yang TL. LDBlockShow: a fast and convenient tool for visualizing linkage disequilibrium and haplotype blocks based on variant call format files. Brief Bioinform. 2021;22:1–6.
50. Otasek D, Morris JH, Boucas J, Pico AR, Demchak B. Cytoscape automation: empowering workflow-based network analysis. Genome Biol. 2019;20:185–99.
51. Shin JH, Blay S, McNeney B, Graham J. LDheatmap: an R function for graphical display of pairwise linkage disequilibria between single nucleotide polymorphisms. J Stat Softw. 2006;16:1–9.
52. Chen H, Patterson N, Reich D. Population di□erentiation as a test for selective sweeps. Genome Res. 2010;20:393–402.
53. Martin SH, Davey JW, Jiggins CD. Evaluating the use of ABBA-BABA statistics to locate introgressed loci. Mol Biol Evol. 2015;32:244–57.
54. Zhao X, Guo Y, Kang L, Yin C, Bi A, Xu D, Zhang Z, Zhang J, Yang X, Xu J, Xu S, Song X, Zhang M, Li Y, Kear P, Wang J, Liu Z, Fu X, Lu F. Genome variation map. 2023. http://bigd.big.ac.cn/gvm/getProjectDetail?project=GVM000463.
55. Assanga SO, Fuentealba M, Zhang G, Tan C, Dhakal S, Rudd JC, Ibrahim AMH, Xue Q, Haley S, Chen J, et al. Mapping of quantitative trait loci for grain yield and its components in a US popular winter wheat TAM 111 using 90K SNPs. PLoS One. 2017;12:1–21.
56. Beales J, Turner A, GriYths S, Snape JW, Laurie DA. A pseudo-response regulator is misexpressed in the photoperiod insensitive *Ppd-D1a* mutant of wheat (*Triticum aestivum* L.). Theor Appl Genet. 2007;115:721–33.
57. Cui F, Zhao C, Ding A, Li J, Wang L, Li X, Bao Y, Li J, Wang H. Construction of an integrative linkage map and QTL mapping of grain yield-related traits using three related wheat RIL populations. Theor Appl Genet. 2014;127:659–75.

58. Gao Y, An K, Guo W, Chen Y, Zhang R, Zhang X, Chang S, Rossi V, Jin F, Cao X, et al. The endosperm-specific transcription factor *TaNAC019* regulates glutenin and starch accumulation and its elite allele improves wheat grain quality. Plant Cell. 2021;33:603–22.
59. Schilling S, Kennedy A, Pan S, Jermiin LS, Melzer R. Genome-wide analysis of MIKC-type MADS-box genes in wheat: pervasive duplications, functional conservation and putative neofunctionalization. New Phytol. 2020;225:511–29.
60. Guan P, Lu L, Jia L, Kabir MR, Zhang J, Lan T, Zhao Y, Xin M, Hu Z, Yao Y, et al. Global QTL analysis identifies genomic regions on chromosomes 4A and 4B harboring stable loci for yield-related traits across di□erent environments in wheat (*Triticum aestivum* L.). Front Plant Sci. 2018;9:529–46.
61. Huang XQ, Cloutier S, Lycar L, Radovanovic N, Humphreys DG, Noll JS, Somers DJ, Brown PD. Molecular detection of QTLs for agronomic and quality traits in a doubled haploid population derived from two Canadian wheats (*Triticum aestivum* L.). Theor Appl Genet. 2006;113:753–66.
62. Kumar A, Mantovani EE, Seetan R, Soltani A, Echeverry-Solarte M, Jain S, Simsek S, Doehlert D, Alamri MS, Elias EM, et al. Dissection of genetic factors underlying wheat kernel shape and size in an elite x nonadapted cross using a high density SNP linkage map. Plant Genome. 2016;9:1–22.
63. Kumar N, Kulwal PL, Gaur A, Tyagi AK, Khurana JP, Khurana P, Balyan HS, Gupta PK. QTL analysis for grain weight in common wheat. Euphytica. 2006;151:135–44.
64. Yan L, Fu D, Li C, Blechl A, Tranquilli G, Bonafede M, Sanchez A, Valarik M, Yasuda S, Dubcovsky J. The wheat and barley vernalization gene *VRN3* is an orthologue of FT. Proc Natl Acad Sci USA. 2006;103:19581–6.
65. Zhang DJ, Zhang XX, Xu W, Hu TT, Ma JH, Zhang YF, Hou J, Hao CY, Zhang XY, Li T. TaGW2L, a GW2-like RING finger E3 ligase, positively regulates heading date in common wheat (*Triticum aestivum* L.). Crop J. 2022;10:972–9.
66. Liu J, Wu BH, Singh RP, Velu G. QTL mapping for micronutrients concentration and yield component traits in a hexaploid wheat mapping population. J Cereal Sci. 2019;88:57–64.
67. Mohler V, Albrecht T, Castell A, Diethelm M, Schweizer G, Hartl L. Considering causal genes in the genetic dissection of kernel traits in common wheat. J Appl Genet. 2016;57:467–76.
68. Moore JW, Herrera-Foessel S, Lan C, Schnippenkoetter W, Ayli□e M, Huerta-Espino J, Lillemo M, Viccars L, Milne R, Periyannan S, et al. A recently evolved hexose transporter variant confers resistance to multiple pathogens in wheat. Nat Genet. 2015;47:1494–8.
69. Paolacci AR, Tanzarella OA, Porceddu E, Varotto S, Cia□ M. Molecular and phylogenetic analysis of MADS-box genes of MIKC type and chromosome location of SEP-like genes in wheat (*Triticum aestivum* L.). Mol Genet Genomics. 2007;278:689–708.
70. Peng J, Richards DE, Hartley NM, Murphy GP, Devos KM, Flintham JE, Beales J, Fish LJ, Worland AJ, Pelica F, et al. 'Green revolution' genes encode mutant gibberellin response modulators. Nature. 1999;400:256–61.
71. Shi WP, Hao CY, Zhang Y, Cheng JY, Zhang Z, Liu J, Yi X, Cheng XM, Sun DZ, Xu YH, et al. A combined association mapping and linkage analysis of kernel number per spike in common wheat (*Triticum aestivum* L.). Front Plant Sci. 2017;8:1412–24.
72. Sun XY, Wu K, Zhao Y, Kong FM, Han GZ, Jiang HM, Huang XJ, Li RJ, Wang HG, Li SS. QTL analysis of kernel shape and weight using recombinant inbred lines in wheat. Euphytica. 2009;165:615–24.
73. Wu QH, Chen YX, Zhou SH, Fu L, Chen JJ, Xiao Y, Zhang D, Ouyang SH, Zhao XJ, Cui Y, et al. High-density genetic linkage map construction and QTL mapping of grain shape and size in the wheat population Yanda 1817 x Beinong6. PLoS One. 2015;10:1–17.
74. Wu XY, Cheng RR, Xue SL, Kong ZX, Wan HS, Li GQ, Huang YL, Jia HY, Jia JZ, Zhang LX, Ma ZQ. Precise mapping of a quantitative trait locus interval for spike length and grain weight in bread wheat (*Triticum aestivum* L.). Mol Breed. 2014;33:129–38.
75. Yao FQ, Li XH, Wang H, Song YN, Li ZQ, Li XG, Gao XQ, Zhang XS, Bie XM. Down-expression of *TaPIN1s* increases the tiller number and grain yield in wheat. BMC Plant Biol. 2021;21:443–53.
76. Han YC, Liu N, Li C, Wang SW, Jia LH, Zhang R, Li H, Tan JF, Xue HW, Zheng WM. *TaMADS2-3D*, a MADS transcription factor gene, regulates phosphate starvation responses in plants. Crop J. 2022;10:243–53.
77. Zhang L, He G, Li Y, Yang Z, Liu T, Xie X, Kong X, Sun J. PIL transcription factors directly interact with SPLs and repress tillering/branching in plants. New Phytol. 2021;233:1414–25.
78. Zikhali M, Wingen LU, Leverington-Waite M, Specel S, Gri□ths S. The identification of new candidate genes *Triticum aestivum* FLOWERING LOCUS T3–B1 (*TaFT3-B1*) and *TARGET* OF EAT1 (*TaTOE1-B1*) controlling the short-day photoperiod response in bread wheat. Plant Cell Environ. 2017;40:2678–90.
79. Acevedo-Garcia J, Spencer D, Thieron H, Reinstadler A, Hammond-Kosack K, Phillips AL, Panstruga R. mlo-based powdery mildew resistance in hexaploid bread wheat generated by a non-transgenic TILLING approach. Plant Biotechnol J. 2017;15:367–78.
80. Carrera A, Echenique V, Zhang W, Helguera M, Manthey F, Schrager A, Picca A, Cervigni G, Dubcovsky J. A deletion at the *Lpx-B1* locus is associated with low lipoxygenase activity and improved pasta color in durum wheat (*Triticum turgidum* ssp *durum*). J Cereal Sci. 2007;45:67–77.
81. Chai L, Xin M, Dong C, Chen Z, Zhai H, Zhuang J, Cheng X, Wang N, Geng J, Wang X, et al. A natural variation in Ribonuclease H-like gene underlies *Rht8* to confer "Green Revolution" trait in wheat. Mol Plant. 2022;15:377–80.
82. Fan M, Miao F, Jia HY, Li GQ, Powers C, Nagarajan R, Alderman PD, Carver BF, Ma ZQ, Yan LL. O-linked N-acetylglucosamine transferase is involved in fine regulation of flowering time in winter wheat. Nat Commun. 2021;12:2303–14.
83. Faris JD, Fellers JP, Brooks SA, Gill BS. A bacterial artificial chromosome contig spanning the major domestication locus Q in wheat and identification of a candidate gene. Genetics. 2003;164:311–21.
84. Guo LJ, Ma M, Wu LN, Zhou MD, Li MY, Wu BW, Li L, Liu XL, Jing RL, Chen W, Zhao H. Modified expression of *TaCYP78A5* enhances grain weight with yield potential by accumulating auxin in wheat (*Triticum aestivum* L.). Plant Biotechnol J. 2022;20:168–82.
85. He XY, Zhang YL, He ZH, Wu YP, Xiao YG, Ma CX, Xia XC. Characterization of phytoene synthase 1 gene (*Psy1*) located on common wheat chromosome 7A and development of a functional marker. Theor Appl Genet. 2008;116:213–21.
86. Himi E, Noda K. Red grain colour gene (*R*) of wheat is a Myb-type transcription factor. Euphytica. 2005;143:239–42.

87. Hou J, Jiang Q, Hao C, Wang Y, Zhang H, Zhang X. Global selection on sucrose synthase haplotypes during a century of wheat breeding. Plant Physiol. 2014;164:1918–29.
88. Jia ML, Li YA, Wang ZY, Tao S, Sun GL, Kong XC, Wang K, Ye XG, Liu SS, Geng SF, et al. TaIAA21 represses TaARF25-mediated expression of *TaERFs* required for grain size and weight development in wheat. Plant J. 2021;108:1754–67.
89. Kong XC, Wang F, Geng SF, Guan JT, Tao S, Jia ML, Sun GL, Wang ZY, Wang K, Ye XG, et al. The wheat *AGL6*-like MADS-box gene is a master regulator for floral organ identity and a target for spikelet meristem development manipulation. Plant Biotechnol J. 2022;20:75–88.
90. Li A, Hao C, Wang Z, Geng S, Jia M, Wang F, Han X, Kong X, Yin L, Tao S, et al. Wheat breeding history reveals synergistic selection of pleiotropic genomic sites for plant architecture and grain yield. Mol Plant. 2022;7:504–19.
91. Li B, Liu D, Li QR, Mao XG, Li A, Wang JY, Chang XP, Jing RL. Overexpression of wheat gene *TaMOR* improves root system architecture and grain yield in Oryza sativa. J Exp Bot. 2016;67:4155–67.
92. Nemoto Y, Kisaka M, Fuse T, Yano M, Ogihara Y. Characterization and functional analysis of three wheat genes with homology to the CONSTANS flowering time gene in transgenic rice. Plant J. 2003;36:82–93.
93. Nilsen KT, Walkowiak S, Xiang DQ, Gao P, Quilichini TD, Willick IR, Byrns B, N'Diaye A, Ens J, Wiebe K, et al. Copy number variation of *TdDof* controls solid-stemmed architecture in wheat. Proc Natl Acad Sci USA. 2020;117:28708–18.
94. Pallotta M, Schnurbusch T, Hayes J, Hay A, Baumann U, Paull J, Langridge P, Sutton T. Molecular basis of adaptation to high soil boron in wheat landraces and elite cultivars. Nature. 2014;514:88–91.
95. Wang W, Pan QL, Tian B, He F, Chen YY, Bai GH, Akhunova A, Trick HN, Akhunov E. Gene editing of the wheat homologs of TONNEAU1-recruiting motif encoding gene a□ects grain shape and weight in wheat. Plant J. 2019;100:251–64.
96. Wei JL, Liao SS, Li MZ, Zhu B, Wang HC, Gu L, Yin HY, Du XY. *AetSRG1* contributes to the inhibition of wheat Cd accumulation by stabilizing phenylalanine ammonia lyase. J Hazard Mater. 2022;428:1–13.
97. Xiao J, Xu SJ, Li CH, Xu YU, Xing LJ, Niu YD, Huan Q, Tang YM, Zhao CP, Wagner D, et al. O-GlcNAc-mediated interaction between VER2 and TaGRP2 elicits *TaVRN1* mRNA accumulation during vernalization in winter wheat. Nat Commun. 2014;5:1–13.